

INTEGRAL SOLUTION FOR THE MICROWAVE BACKGROUND ANISOTROPIES IN NONFLAT UNIVERSES

MATIAS ZALDARRIAGA

Department of Physics, MIT, Cambridge, MA 02139

UROŠ SELJAK

Harvard Smithsonian Center for Astrophysics, Cambridge, MA 02138

AND

EDMUND BERTSCHINGER

Department of Physics, MIT, Cambridge, MA 02139

Received 1997 April 28; accepted 1997 October 1

ABSTRACT

We present an efficient method of computing cosmic microwave background (CMB) anisotropies in nonflat universes. First, we derive the Boltzmann equation for CMB temperature and polarization fluctuations produced by scalar perturbations in a general Robertson-Walker universe. We then apply the integral method in order to solve this equation, writing temperature and polarization anisotropies as a time integral over a geometrical term and a source term. The geometrical terms can be written using ultraspherical Bessel functions, which depend on curvature. These cannot be precomputed, as for flat space. Instead, we solve their differential equation directly for selected values of the multipoles. The resulting computational time is comparable to the flat-space case, improving over previous methods by 2–3 orders of magnitude. This allows one to compute highly accurate CMB temperature and polarization spectra, matter transfer functions, and their CMB normalizations for any cosmological model, thereby avoiding the need to use the various inexact fitting formulae that exist in the literature.

Subject headings: cosmic microwave background — dark matter — gravitation — large-scale structure of universe

1. INTRODUCTION

In the past few years the field of cosmic microwave background (CMB) anisotropies has been transformed from a theoretical exercise to an active experimental area of research. Since their first discovery by *COBE* in 1992 (Smoot et al. 1992), there have been more than a dozen independent detections of fluctuations over a much larger angular range (see, e.g., Lineweaver et al. 1996; Rocha & Hancock 1996 for compilations). The future looks even more promising, as there are two funded satellite missions in planning, one in Europe (*Planck*) and one in the US (*MAP*), that promise to measure the anisotropies to an exquisite accuracy over three decades in angular scale. This will open the possibility of determining many cosmological parameters with much greater accuracy than any other probe in cosmology (Jungman et al. 1996; Bond, Efstathiou, & Tegmark 1997; Zaldarriaga, Spergel, & Seljak 1996).

In light of this experimental promise, theoretical predictions have been advanced to a higher stage as well. It is not sufficient any longer to make qualitative statements and approximate predictions for analyzing the forthcoming data and guiding experimental design. Rather, what is needed are very accurate predictions of CMB spectra (typically to better than 1%), which allow one to study the CMB sensitivity to various cosmological parameters. Because this sensitivity depends on the choice of mission specifics, such as number of detectors, their noise characteristics, or angular resolution, it is important that such accurate predictions be available already at the mission design stage, when its characteristics are still open to modification. In Seljak & Zaldarriaga (1996, hereafter Paper I) we presented a method that is both fast, accurate, and applicable to any flat cosmological model. The method is based on the

source time integration over the photon past light cone, and it has the advantage of reducing the computational time by about 2 orders of magnitude, compared to the more traditional methods, while still being exact, in the sense that it can achieve arbitrary precision within the limits of linear perturbation theory. Such a method therefore allows one to explore a large range of parameter space with high accuracy.

Open cosmological models and their predictions for the CMB have received much attention lately (e.g., Gouda & Sugiyama 1992; Kamionkowski, Spergel, & Sugiyama 1994; Hu, Bunn, & Sugiyama 1995; White & Bunn 1996; Gorski et al. 1995). The reason for this is simple: observational evidence from the nearby universe (e.g., Peebles 1993) suggests that an open universe is favored over the critical or closed one. While the differences might be resolved with the addition of a cosmological constant Λ , so that the geometry of the universe would remain flat, the value of Λ is already significantly constrained by a number of independent tests based on *COBE* data, lensing statistics, and SN Type Ia results (Bunn & White 1997; Kochanek 1996; Perlmutter et al. 1996). It therefore seems natural to explore the possibility that the universe is indeed open. From a theoretical point of view, open inflationary models proved to be constructive and capable of generating the initial perturbations (e.g., Lyth & Stewart 1990; Ratra & Peebles 1994; Liddle et al. 1995; Bucher, Goldhaber, & Turok 1995). Models with positive curvature, although currently less popular, have also been studied in detail (White & Scott 1996).

All the computations of CMB anisotropies in open and closed universes carried out so far have used the traditional Boltzmann hierarchy approach pioneered by Peebles & Yu

(1970) and extended by Wilson & Silk (1981) and Bond & Efstathiou (1984). The speed limitations of the Boltzmann approach in flat space were extensively discussed in Paper I. In the case of nonflat geometry they become even worse: solving the hierarchy in an open universe is much slower than in the flat case, and it leads to extremely long integration times. This makes an accurate search over a large set of parameter space practically impossible. Instead, one is forced to use approximations, but, as shown in this paper, these give at best a few percent accuracy and can be very misleading in the study of parameter determination.

In this paper we develop the integral solution for photon transport in a general Robertson-Walker background, thereby generalizing the method developed in Paper I to a nonflat geometry. As in the flat case, the solution is written in terms of a time integral over a source term and a geometrical term. The latter can be expressed in terms of ultraspherical Bessel functions, defined as the radial part of the eigenfunction of the Laplacian on a curved manifold. We present a method for computing these functions efficiently in the context of CMB calculations and incorporate them into the integral solution. This allows us to achieve a fast and accurate method, improving over previous calculational methods by 2–3 orders of magnitude. In this paper we concentrate on the temperature and polarization anisotropies produced by scalar modes; the generalization to vector and tensor perturbations will be presented elsewhere (Hu et al. 1997). The outline of the paper is as follows: In § 2 we present the Einstein and fluid equations in a general Robertson-Walker background. In § 3 we discuss the Boltzmann hierarchy for CMB photons, and in § 4 we derive its integral solution. In § 5 we discuss in detail the method for computing the ultraspherical Bessel functions. The comparison between the exact solution and the approximations often used in the literature is presented in § 6. In § 7 we discuss the numerical implementation of the method. This is followed by discussion and conclusions in § 8. In an Appendix we present an alternative derivation of the integral solution, highlighting its geometrical interpretation.

2. EINSTEIN AND FLUID EQUATIONS

In this section we present the Einstein and fluid differential equations for the metric, cold dark matter (CDM), and baryons that must be solved to calculate the CMB anisotropy spectra. These equations are the basis of the traditional methods and are also used in the integral method, discussed in § 4. The derivation of the Einstein and fluid equations in a nonflat background can be found in the literature (see, for example, Bertschinger 1996), so we just present the final results.

The metric is written as

$$\begin{aligned} ds^2 &= -dt^2 + a^2(\gamma_{ij} + h_{ij})dx^i dx^j \\ &= a^2[-d\tau^2 + (\gamma_{ij} + h_{ij})dx^i dx^j], \end{aligned} \quad (1)$$

where a is the expansion factor, x_i are the comoving coordinates, and $\tau = \int dt/a$ is the conformal time. We are using units in which $c = 1$. The space part of the unperturbed metric is γ_{ij} with constant curvature $K = H_0^2(\Omega_0 - 1)$, and h_{ij} is the metric perturbation in synchronous gauge (Lifshitz 1946). Although all observable quantities are identical in different gauges, the computational efficiency of obtaining them within a given accuracy is not. This criterion leads us

to work in synchronous gauge.¹ In comparison with the longitudinal gauge (Bardeen 1980), the latter is about 20% more efficient with isentropic initial conditions, and even more so with isocurvature initial conditions, which are difficult to set up in the longitudinal gauge.

When working with linear theory in a flat universe, it is convenient to use Fourier modes, as they evolve independently. Their generalization in a nonflat universe is the eigenfunctions of the Laplacian operator, which we shall call $G(k, x)$ (e.g., Abbott & Schaefer 1986),

$$\nabla^2 G(k, x) = -k^2 G(k, x). \quad (2)$$

We expand all the perturbations in terms of G and its spatial covariant derivatives. For example, the metric perturbations for a single mode are given by

$$h_{ij} = \frac{h}{3} \gamma_{ij} G + (h + 6\eta) \left(k^{-2} G_{|ij} + \frac{1}{3} \gamma_{ij} G \right), \quad (3)$$

where h and $h + 6\eta$ are the trace and traceless part of the metric perturbation. Covariant derivatives with respect to the metric γ_{ij} are denoted by a $.$. The perturbed Einstein's equations result in the following equations for h and η (Bertschinger 1996):

$$\begin{aligned} (k^2 - 3K)\eta - \frac{1}{2} \frac{\dot{a}}{a} \dot{h} &= -8\pi \mathcal{G} a^2 \delta\rho, \\ (k^2 - 3K)\dot{\eta} + \frac{K}{2} \dot{h} &= 4\pi \mathcal{G} a^2 (\bar{\rho} + \bar{p})kv. \end{aligned} \quad (4)$$

\mathcal{G} here stands for the gravitational constant; $\delta\rho$ and v characterize the density and velocity perturbations ($v = i\hat{k} \cdot v$), $\delta\rho = \sum_j \bar{\rho}_j \delta_j$, and $(\bar{\rho} + \bar{p})v = \sum_j (\bar{\rho}_j + \bar{p}_j)v_j$, where $\bar{\rho}_j$ and \bar{p}_j are the mean density and pressure of the j th species, respectively, and the sum is carried out over all the different species in the universe.

The equation for the CDM density perturbation δ_c is

$$\dot{\delta}_c = -\frac{\dot{h}}{2}, \quad (5)$$

where, by definition, in this gauge the CDM particles have zero peculiar velocities. The Euler equation for the baryons has additional terms caused by Thomson scattering and pressure, so baryons have velocities relative to the dark matter of

$$\begin{aligned} \dot{\delta}_b &= -kv_b - \frac{\dot{h}}{2}, \\ \dot{v}_b &= -\frac{\dot{a}}{a} v_b + c_s^2 k \delta_b + \frac{4\bar{\rho}_\gamma}{3\bar{\rho}_b} a n_e x_e \sigma_T (v_\gamma - v_b). \end{aligned} \quad (6)$$

Here, c_s is the baryon sound speed, v_b is the baryon velocity, v_γ is given by the temperature dipole $v_\gamma = 3\Delta_{T1}$, and $\bar{\rho}_\gamma$ and $\bar{\rho}_b$ are the mean photon and baryon densities, respectively. The Thomson scattering cross section is σ_T , n_e is the electron density, and x_e is the ionization fraction.

3. BOLTZMANN EQUATION

In this section we discuss CMB anisotropies and present a derivation of the Boltzmann equation for the photons. Because we use a novel approach to treat this problem (see also Hu & White 1997), we begin by considering flat geometries in § 3.1, then generalize the results to arbitrary

¹ In Paper I we presented the equations in the longitudinal gauge.

Robertson-Walker backgrounds in § 3.2. The derivation of the Boltzmann hierarchy for polarization is new work. The notation that we use is largely based on Paper I.

The CMB radiation field is described by a 2×2 intensity tensor I_{ij} (Chandrasekhar 1960). The Stokes parameters Q and U are defined as $Q = (I_{11} - I_{22})/4$ and $U = I_{12}/2$, while the temperature anisotropy is given by $T = (I_{11} + I_{22})/4$. The fourth Stokes parameter V that describes circular polarization is not necessary in standard cosmological models, because it cannot be generated through the process of Thomson scattering. While the temperature is a scalar quantity, Q and U are not. They depend on the direction of observation \hat{n} and on the two axes (\hat{e}_1, \hat{e}_2) perpendicular to \hat{n} that are used to define them. If for a given \hat{n} , the axes (\hat{e}_1, \hat{e}_2) are rotated by an angle ψ , such that $\hat{e}'_1 = \hat{e}_1 \cos \psi + \hat{e}_2 \sin \psi$ and $\hat{e}'_2 = \hat{e}_1(-\sin \psi) + \hat{e}_2 \cos \psi$, the Stokes parameters change as

$$\begin{aligned} Q' &= U \cos 2\psi + U \sin 2\psi, \\ U' &= Q(-\sin 2\psi) + U \cos 2\psi. \end{aligned} \quad (7)$$

To analyze the CMB temperature on the sky, it is natural to expand it in spherical harmonics. These are not appropriate for polarization, because the two combinations $Q \pm iU$ are quantities of spin ± 2 (Goldberg et al. 1967). They should be expanded in spin-weighted harmonics ${}_{\pm 2}Y_l^m$ (Zaldarriaga & Seljak 1997),

$$\begin{aligned} T(\hat{n}) &= \sum_{lm} a_{T,lm} Y_{lm}(\hat{n}), \\ (Q + iU)(\hat{n}) &= \sum_{lm} a_{2,lm} Y_{lm}(\hat{n}), \\ (Q - iU)(\hat{n}) &= \sum_{lm} a_{-2,lm} Y_{lm}(\hat{n}). \end{aligned} \quad (8)$$

There is an equivalent expansion using tensors on the sphere (Kamionkowski, Kosowsky, & Stebbins 1997). The coefficients $a_{\pm 2,lm}$ are observable on the sky, and their power spectra can be predicted for different cosmological models. Instead of $a_{\pm 2,lm}$, it is convenient to use their linear combinations $a_{E,lm} = -(a_{2,lm} + a_{-2,lm})/2$ and $a_{B,lm} = -(a_{2,lm} - a_{-2,lm})/2i$, which have opposite parities. Four power spectra are needed to characterize fluctuations in a Gaussian theory, the autocorrelation of T , E , and B , and the cross-correlation of E and T . Because of parity considerations, the cross-correlations between B and the other quantities vanish, and one is left with

$$\begin{aligned} C_{XI} &= \frac{1}{2l+1} \sum_m \langle a_{X,lm}^* a_{X,lm} \rangle, \\ C_{CI} &= \frac{1}{2l+1} \sum_m \langle a_{T,lm}^* a_{E,lm} \rangle, \end{aligned} \quad (9)$$

where X stands for T , E , or B , and $\langle \dots \rangle$ means ensemble average. Only vector and tensor modes contribute to B (Zaldarriaga & Seljak 1997; Kamionkowski et al. 1997), hence we may ignore it in the remainder of this paper.

3.1. Flat Geometry

We will begin by studying perturbations in a flat universe in order to introduce our notation and clarify the treatment of polarization, which differs from the usual method, in which Legendre polynomials are used to expand both temperature and polarization (e.g., Bond & Efstathiou 1984). As we are dealing with a linear problem, we may consider only

one eigenmode of the Laplacian (a plane wave in the flat case) at a time. We may choose $\mathbf{k} \parallel \hat{z}$ without loss of generality. To define the Stokes parameters, we use the spherical coordinate unit vectors $(\hat{e}_\theta, \hat{e}_\phi)$. In this particular coordinate system, only Q is different from zero, and we denote it by Δ_P , so that $\Delta_P = Q = Q \pm iU (U=0)$. The temperature anisotropy for the single eigenmode is denoted by Δ_T .

For a single plane wave, rotational symmetry implies that both Δ_T and Δ_P depend only on the angle between \hat{n} and \hat{z} ($\mathbf{k} \parallel \hat{z}$), so only harmonics with $m=0$ are needed in the expansion. To calculate the evolution of these two quantities, we expand them as

$$\begin{aligned} \Delta_T(\mathbf{k}, \hat{n}) &= G(\mathbf{k}, x) \sum_l (-i)^l \sqrt{4\pi(2l+1)} \Delta_{Tl} Y_l^0 \\ &= G(\mathbf{k}, x) \sum_l (-i)^l (2l+1) \Delta_{Tl} P_l(\mu), \\ \Delta_P &= G(\mathbf{k}, x) \sum_l (-i)^l \\ &\quad \times \sqrt{4\pi(2l+1)(l+2)!/(l-2)!} \Delta_{Pl2} Y_l^0(\mu) \\ &= G(\mathbf{k}, x) \sum_l (-i)^l \\ &\quad \times \sqrt{4\pi(2l+1)(l+2)!/(l-2)!} \Delta_{Pl-2} Y_l^0(\mu) \\ &= G(\mathbf{k}, x) \sum_l (-i)^l (2l+1) \Delta_{Pl} P_l^2(\mu), \end{aligned} \quad (10)$$

where $G(\mathbf{k}, x) = \exp(i\mathbf{k} \cdot \mathbf{x})$ and $\mu = \hat{\mathbf{k}} \cdot \hat{\mathbf{n}}$. We added a sub-index ± 2 to $\Delta_{Pl\pm 2}$ to denote that they are the expansion coefficients in spin ± 2 harmonics,² and we used the explicit expression for spin- s harmonics with $m=0$ in order to write them in terms of associated Legendre polynomials (Goldberg et al. 1967),

$$\begin{aligned} Y_l^0(\theta, \phi) &= \sqrt{\frac{(2l+1)}{4\pi}} P_l(\cos \theta), \\ {}_{\pm 2}Y_l^0(\theta, \phi) &= \sqrt{\frac{(2l+1)(l-2)!}{4\pi(l+2)!}} P_l^2(\cos \theta). \end{aligned} \quad (11)$$

As stated above, for scalar modes in this reference frame $U=0$, so Δ_P describes both spin ± 2 quantities. For $m=0$, one has ${}_2Y_l^0 = {}_{-2}Y_l^0$, and so, ${}_2\Delta_{Pl} = {}_{-2}\Delta_{Pl}$. For density perturbations, only $m=0$ harmonics are needed in the expansion, because of the azimuthal symmetry, but the treatment can be generalized to vector and tensor modes. In these cases, modes with $m=\pm 1$ and $m=\pm 2$ are required, respectively. For vector and tensor modes, U is no longer zero, so separate expansions for both $Q+iU$ and $Q-iU$ are needed.

The Boltzmann equation for the CMB photons reads (e.g., Ma & Bertschinger 1995),

$$\begin{aligned} \dot{\Delta}_T + ik\mu \Delta_T &= -\frac{1}{6}\dot{h} - \frac{1}{6}(\dot{h} + 6\dot{\eta})P_2(\mu) + \dot{\Delta}_{T|Tho} \\ \dot{\Delta}_P + ik\mu \Delta_P &= \dot{\Delta}_{P|Tho}. \end{aligned} \quad (12)$$

The first term in the temperature equation represents the effect of gravitational redshift, while $\dot{\Delta}_{T|Tho}$ and $\dot{\Delta}_{P|Tho}$ are the changes in the photon distribution function produced by Thomson scattering, where the derivatives are taken with respect to conformal time. After inserting equation (10)

² The relation between these coefficient and those used in Zaldarriaga & Seljak (1997) is ${}_{\pm 2}\Delta_{Pl} = -\sqrt{(l-2)!/(l+2)!} \Delta_{El}$.

into equation (12), one obtains a system of two coupled hierarchies,

$$\begin{aligned}\dot{\Delta}_{T0} &= -k \Delta_{T1} - \frac{\hbar}{6} + \dot{\Delta}_{T0|_{\text{Tho}}}, \\ \dot{\Delta}_{T1} &= \frac{k}{3} (\Delta_{T0} - 2 \Delta_{T2}) + \dot{\Delta}_{T1|_{\text{Tho}}}, \\ \dot{\Delta}_{T2} &= \frac{k}{5} [2 \Delta_{T1}^{(S)} - 3 \Delta_{T3}] + \frac{2}{15} k^2 \alpha + \dot{\Delta}_{T2|_{\text{Tho}}}, \\ \dot{\Delta}_{Tl} &= \frac{k}{2l+1} [l \Delta_{T(l-1)} - (l+1) \Delta_{T(l+1)}] \\ &\quad + \dot{\Delta}_{Tl|_{\text{Tho}}}, \quad l > 2, \\ \dot{\Delta}_{Pl2} &= \frac{k}{2l+1} [(l-2) \Delta_{Pl-12} - (l+3) \Delta_{Pl+1}] \\ &\quad + \dot{\Delta}_{Pl|_{\text{Tho}}},\end{aligned}\quad (13)$$

where $\alpha = (\hbar + 6\eta)/2k^2$, and we used the recurrence relations for the Legendre functions,

$$\begin{aligned}\mu P_l(\mu) &= \frac{1}{2l+1} [l P_{l-1} + (l+1) P_{l+1}], \\ \mu P_l^2(\mu) &= \frac{1}{2l+1} [(l+2) P_{l-1}^2 + (l-1) P_{l+1}^2].\end{aligned}\quad (14)$$

The Thomson scattering cross section is

$$\frac{d\sigma}{d\Omega} = \frac{3\sigma_T}{8\pi} |\tilde{\epsilon} \cdot \tilde{\epsilon}'|^2, \quad (15)$$

where $\tilde{\epsilon}$ and $\tilde{\epsilon}'$ are the unit vectors that describe the polarization of the electric field of the scattered and incoming radiation, respectively. The scattering terms in equations (13) are most easily computed in the coordinate system in which the incident photons travel along the \hat{z} -axis and the electrons are at rest. If \hat{n}' is the direction of the incident photon, and \hat{n} is that of the scattered one, then $\hat{n}' = \hat{z} = (\theta = 0, \phi = 0)$ and (θ, ϕ) describe \hat{n} . For a given scattering event, the Thomson scattering matrix is the simplest when expressed in terms of the intensities of radiation parallel (\tilde{T}_{\parallel}) and perpendicular (\tilde{T}_{\perp}) to the plane containing both \hat{n} and \hat{n}' . Equation (15) leads to the following relation between incoming and scattered radiation:

$$\begin{aligned}\tilde{T}_{\parallel} &= \frac{3}{8\pi} \sigma_T \tilde{T}'_{\parallel} \cos^2 \theta, \\ \tilde{T}_{\perp} &= \frac{3}{8\pi} \sigma_T \tilde{T}'_{\perp}, \\ \tilde{U} &= \frac{3}{8\pi} \sigma_T \tilde{U}' \cos \theta,\end{aligned}\quad (16)$$

where σ_T is the Thomson scattering cross section. The total intensity is the sum of the two components, $\tilde{T} = \tilde{T}_{\parallel} + \tilde{T}_{\perp}$, while the difference gives polarization $\tilde{Q} = \tilde{T}_{\parallel} - \tilde{T}_{\perp}$. Because the components are measured using this coordinate system, the Stokes parameters of the incoming radiation \tilde{Q}' and \tilde{U}' depend on the angle ϕ of the scattered photon, while \tilde{Q} and \tilde{U} are already measured relative to the

correct frame. It is more useful to refer the Stokes parameters of the incoming radiation relative to a fixed frame. To achieve this, we construct the scattering matrix in terms of T' , $Q' + iU' = (\exp 2i\phi)(\tilde{Q}' + i\tilde{U}')$ and $Q' - iU' = (\exp -2i\phi)(\tilde{Q}' - i\tilde{U}')$, where we have used the transformation law (eq. [7]) to relate the two sets of Stokes parameters.

Equation (16) implies that the scattered radiation in direction \hat{n} is

$$\begin{aligned}\delta T(\hat{n}', \hat{n}) &= \frac{\sigma_T}{4\pi} \left[\frac{3}{4} (1 + \cos^2 \theta) T' + \frac{3}{8} (\cos^2 \theta - 1) \right. \\ &\quad \times e^{-2i\phi} (Q' + iU') + \frac{3}{8} (\cos^2 \theta - 1) e^{2i\phi} (Q' - iU') \Big], \\ \delta(Q \pm iU)(\hat{n}', \hat{n}) &= \frac{\sigma_T}{4\pi} \left[\frac{3}{4} (\cos^2 \theta - 1) T' + \frac{3}{8} \right. \\ &\quad \times (\cos \theta \pm 1)^2 e^{-2i\phi} (Q' + iU') + \frac{3}{8} \\ &\quad \times (\cos \theta \mp 1)^2 e^{2i\phi} (Q' - iU') \Big].\end{aligned}\quad (17)$$

The final expression for the scattered field is an integral over all directions \hat{n}' :

$$\dot{X}(\hat{n})|_{\text{Tho}} = -a \sigma_T n_e x_e \left[X(\hat{n}) + \int d\Omega' \delta X(\hat{n}', \hat{n}) \right], \quad (18)$$

where X stands for T and $Q \pm iU$. The first term accounts for the photons that are scattered away from the line of sight, and the expansion factor a is introduced because we are calculating the derivative with respect to conformal time.

Equation (17) for the scattering matrix is written in the frame where $\hat{n}' = (\theta' = 0, \phi' = 0)$. We can use equation (11) to show that ${}_{\pm 2}Y_2^2(\hat{n}) = (1/4\pi)^{1/2} (1 \mp \cos \theta)^2 / 2e^{2i\phi}$ and ${}_{\pm 2}Y_2^{-2}(\hat{n}) = (1/4\pi)^{1/2} (1 \pm \cos \theta)^2 / 2e^{-2i\phi}$. These, together with the explicit expressions $\partial Y_{00}^m(\hat{n}) = 1/4\pi \delta_{m0}$, ${}_0Y_2^m(\hat{n}) = (5/4\pi)^{1/2} \delta_{m0}$, and ${}_{\pm 2}Y_2^m(\hat{n}) = (5/4\pi)^{1/2} \delta_{m\mp 2}$, enable us to rewrite equation (17) in a more useful form (δ_{ij} is the Kronecker delta):

$$\begin{aligned}\delta T(\hat{n}', \hat{n}) &= \sigma_T \sum_m \{ [{}_{10}{}_0Y_2^m(\hat{n}) {}_0\bar{Y}_2^m(\hat{n}') \\ &\quad + {}_0Y_0^m(\hat{n}) {}_0\bar{Y}_0^m(\hat{n}')] T' \\ &\quad + \frac{3}{20} \sqrt{\frac{2}{3}} {}_0Y_2^m(\hat{n}) {}_2\bar{Y}_2^m(\hat{n}') (Q' + iU') \\ &\quad - \frac{3}{20} \sqrt{\frac{2}{3}} {}_0Y_2^m(\hat{n}) {}_{-2}\bar{Y}_2^m(\hat{n}') (Q' - iU') \}, \\ \delta(Q \pm iU)(\hat{n}', \hat{n}) &= \sigma_T \sum_m \left[-\frac{6}{20} {}_{\pm 2}Y_2^m(\hat{n}) {}_0\bar{Y}_2^m(\hat{n}') T' \right. \\ &\quad + \frac{6}{20} {}_{\pm 2}Y_2^m(\hat{n}) {}_2\bar{Y}_2^m(\hat{n}') (Q' + iU') \\ &\quad \left. + \frac{6}{20} Y_2^m(\hat{n}) {}_{-2}\bar{Y}_2^m(\hat{n}') (Q' - iU') \right].\end{aligned}\quad (19)$$

The advantage of this form for the scattering matrix comes from the fact that we want the scattering matrix in the frame in which $k \parallel \hat{z}$, and not $\hat{n}' = \hat{z}$. The sum $\sum_m {}_sY_l^m(\hat{n}) {}_s\bar{Y}_l^m(\hat{n}')$ acquires a phase change under rotation of the coordinate system that exactly cancels the phase change in the transformation of $Q \pm iU$ in equation (19). We may therefore use this equation in the coordinate system where $k \parallel \hat{z}$ to compute the Thomson scattering terms in equation (13). Equation (19) is also particularly useful in performing the integral in equation (18).

Substituting the expansion for the Stokes parameters from equation (10) into equation (19), and using equation (18), we find

$$\begin{aligned}\Delta_{Tl}|_{\text{Tho}} &\equiv -a\sigma_T n_e x_e \left[\Delta_{Tl} + \int d\Omega_0 Y_l^m(\hat{n}) \delta T(\hat{n}) \right] \\ &= \dot{\kappa} \left(-\Delta_{Tl} + \Delta_{T0} \delta_{l0} + \frac{\Pi}{10} \delta_{l2} \right) \\ {}_{\pm 2}\Delta_{Pl}|_{\text{Tho}} &\equiv -a\sigma_T x_e n_e \left[{}_{\pm 2}\Delta_{Pl} + \int d\Omega_2 Y_l^m(\hat{n}) \delta \right. \\ &\quad \times (Q \pm iU)(\hat{n}) \left. \right] \\ &= \dot{\kappa} \left({}_{\pm 2}\Delta_{Pl} - \frac{\Pi}{20} \delta_{l2} \right),\end{aligned}\quad (20)$$

with $\Pi = \Delta_{T2} - 6({}_2\Delta_{Pl} + {}_{-2}\Delta_{Pl})$. The differential optical depth for Thomson scattering is denoted by $\dot{\kappa} = an_e x_e \sigma_T$. Note that the polarization has sources only at $l = 2$. One can apply the same analysis to vector and tensor perturbations, the only difference being that in equation (10), the expansion is in terms of harmonics with $m = \pm 1, \pm 2$ for vectors and tensors, respectively. In fact, the form of the scattering terms in equation (20) is the same for the three types of perturbations, as also noted by Hu & White (1997). Equation (20) is valid in the rest frame of the electrons, so in the reference frame where the baryon velocity is v_b , the distribution of scattered radiation has an additional dipole. The final expression for the Boltzmann hierarchy is

$$\begin{aligned}\Delta_{T0} &= -k\Delta_{T1} - \frac{\dot{h}}{6} \\ \Delta_{T1} &= \frac{k}{3} (\Delta_{T0} - 2\Delta_{T2}) + \dot{\kappa} \left(\frac{v_b}{3} - \Delta_{T1} \right) \\ \Delta_{T2} &= \frac{k}{5} [2\Delta_{T1}^{(S)} - 3\Delta_{T3}] + \frac{2}{15} k^2 \alpha + \dot{\kappa} \left(\frac{\Pi}{10} - \Delta_{T2} \right) \\ \Delta_{Tl} &= \frac{k}{2l+1} [l\Delta_{T(l-1)} - (l+1)\Delta_{T(l+1)}] \\ &\quad - \dot{\kappa} \Delta_{Tl} \quad l > 2, \\ {}_2\Delta_{Pl} &= \frac{k}{2l+1} [(l-2){}_2\Delta_{P(l-1)} - (l+3){}_2\Delta_{P(l+1)}] \\ &\quad - \dot{\kappa} {}_2\Delta_{Pl} - \frac{1}{20} \dot{\kappa} \Pi \delta_{l2}.\end{aligned}\quad (21)$$

3.2. Nonflat Geometry

We now proceed to generalize the results of the § 3.1 to a general Robertson-Walker background. First, we generalize equation (21). Following Wilson & Silk (1981), we expand the photon temperature Δ_T in terms of Legendre tensors,

$$\Delta_T = \sum_l (2l+1) \Delta_{Tl} (-\beta)^{-l} \left(\prod_l b_l \right)^{-1} G_{|i_1 \dots i_l} P_l^{i_1 \dots i_l}, \quad (22)$$

with $\beta^2 = k^2 + K$, $b_l^2 = 1 - Kl^2/\beta^2$, and $|i_1 \dots i_l$ covariant derivatives. These Legendre tensors are symmetric combinations constructed out of \hat{n} and the metric g^{ij} , using the

recursion

$$(2l+1)\hat{n}^i P_l^{i_1 \dots i_l} = (l+1)P_{l+1}^{i_1 \dots i_{l+1}} + l g^{(i i_1} P_{l-1}^{i_2 \dots i_l)}, \quad (23)$$

where the parentheses imply symmetrization with respect to the indices (Wilson & Silk 1981; White & Scott 1995). The first moment at $l = 0$ is given by $P_0 = 1$. In the flat universe this recursion reduces to equation (14), and equation (22) is equivalent to equation (10).

To generalize equation (10) to polarization, the Legendre tensors should be constructed in a different way. Polarization depends both on \hat{n} and on (\hat{e}_1, \hat{e}_2) in the plane perpendicular to it. One may form the linear combination $\hat{m} = 2^{-1/2}(\hat{e}_1 + i\hat{e}_2)$ and construct the appropriate tensors by combining \hat{n} and \hat{m} . We expand the polarization perturbation as

$$\Delta_P = \sum_l (2l+1) {}_2\Delta_{Pl} (-\beta)^{-l} \left(\prod_l b_l \right)^{-1} G_{|i_1 \dots i_l 2} P_l^{i_1 \dots i_l}. \quad (24)$$

These “spin” Legendre tensors are symmetric combinations constructed out of \hat{n} , \hat{m} , and the metric g^{ij} , using the recurrence

$$(2l+1)\hat{n}^{(i_2} P_l^{i_1 \dots i_l)} = (l-1)P_{l+1}^{i_1 \dots i_{l+1}} + (l+2)g^{(i i_1} P_{l-1}^{i_2 \dots i_l)}. \quad (25)$$

The hierarchy begins at $l = 2$ with ${}_2P_2^{ij} = 3m^i m^j$. To derive the Boltzmann hierarchies for polarization, the following properties are useful and can be proven by induction:

$$\begin{aligned}g_{i_1 i_2} P_l^{i_1 \dots i_l} &= 0 \quad g_{i_1 i_2 2} P_l^{i_1 \dots i_l} = 0 \\ \hat{n}_{i_1} P_l^{i_1 \dots i_l} &= P_{l-1}^{i_1 \dots i_{l-1}} \hat{n}_{i_1} {}_2P_l^{i_1 \dots i_l} = (l+2) {}_2P_{l-1}^{i_1 \dots i_{l-1}} / l.\end{aligned}\quad (26)$$

Using equations (23), (25), and (26) we obtain

$$\begin{aligned}G_{|i_1 \dots i_l} \hat{n}^i P_l^{i_1 \dots i_l} &= \frac{1}{(2l+1)} [-(l+1)G_{|i_1 \dots i_{l+1}} P_l^{i_1 \dots i_{l+1}} \\ &\quad + l\beta^2 b_l^2 G_{|i_1 \dots i_{l-1}} P_l^{i_1 \dots i_{l-1}}], \\ G_{|i_1 \dots i_l} \hat{n}^i {}_2P_l^{i_1 \dots i_l} &= \frac{1}{(2l+1)} [-(l+3)G_{|i_1 \dots i_{l+1} 2} P_l^{i_1 \dots i_{l+1}} \\ &\quad + (l-2)\beta^2 b_l^2 G_{|i_1 \dots i_{l-1} 2} P_l^{i_1 \dots i_{l-1}}].\end{aligned}\quad (27)$$

These relations, together with

$$\begin{aligned}\int d\Omega \int dV (G_{|i_1 \dots i_l} P_{l-1}^{i_1 \dots i_l} G_{|i_1 \dots i_{l-1}} P_{l-1}^{i_1 \dots i_{l-1}})_{|i} n^i &= 0, \\ \int d\Omega \int dV (G_{|i_1 \dots i_l 2} P_l^{i_1 \dots i_l} G_{|i_1 \dots i_{l-1} 2} P_{l-1}^{i_1 \dots i_{l-1}})_{|i} n^i &= 0,\end{aligned}\quad (28)$$

can be used to show that our choice of normalization in equations (23) and (25) coincides with that of flat space.

The Boltzmann equation,

$$\begin{aligned}\dot{\Delta}_T + n^i \Delta_{T|i} &= -\frac{1}{6}(\dot{h} + G_{|ij} P_2^{ij}) + \dot{\Delta}_{T|\text{Tho}}, \\ \dot{\Delta}_P + n^i \Delta_{P|i} &= \dot{\Delta}_{P|\text{Tho}},\end{aligned}\quad (29)$$

now becomes a hierarchy:

$$\begin{aligned}
 \dot{\Delta}_{T0} &= -k \Delta_{T1} - \frac{\dot{h}}{6}, \\
 \dot{\Delta}_{T1} &= \frac{\beta}{3} (b_1 \Delta_{T0} - 2b_2 \Delta_{T2}) + \dot{\kappa} \left(\frac{v_b}{3} - \Delta_{T1} \right), \\
 \dot{\Delta}_{T2} &= \frac{\beta}{5} (2b_2 \Delta_{T1} - 3b_3 \Delta_{T3}) + \frac{2}{15} k^2 \bar{b} \alpha + \dot{\kappa} \left(\frac{\Pi}{10} - \Delta_{T2} \right), \\
 \dot{\Delta}_{Tl} &= \frac{\beta}{2l+1} [l b_l \Delta_{T(l-1)} - (l+1) b_{l+1} \Delta_{T(l+1)}] \\
 &\quad - \dot{\kappa} \Delta_{Tl}, \quad l > 2, \\
 {}_2\dot{\Delta}_{Pl} &= \frac{\beta}{2l+1} [(l-2) b_{l-2} \Delta_{Pl-1} - (l+3) b_{l+1} {}_2\Delta_{Pl+1}] \\
 &\quad - \dot{\kappa} {}_2\Delta_{Pl} - \frac{1}{20} \dot{\kappa} \Pi \delta_{l2}, \quad (30)
 \end{aligned}$$

where $\Pi = \Delta_{T2} - 12 {}_2\Delta_{Pl}$, and $\bar{b} = (1 - 3K/k^2)^{1/2} = \beta b_2/k$. The same hierarchy (eq. [30]), but without Thomson scattering and polarization, applies to massless neutrinos, while for massive neutrinos, the hierarchy depends on the momentum as well (e.g., Ma & Bertschinger 1995).

Finally, the power spectra are given by

$$\begin{aligned}
 C_{(T,E)l} &= (4\pi)^2 \int \beta^2 d\beta P(\beta) |\Delta_{(T,E)l}(\beta, \tau = \tau_0)|^2, \\
 C_{Cl} &= (4\pi)^2 \int \beta^2 d\beta P(\beta) \Delta_{Tl}(\beta, \tau = \tau_0) \Delta_{El}(\beta, \tau = \tau_0), \\
 \Delta_{El} &= - \sqrt{\frac{(l+2)!}{(l-2)!}} {}_2\Delta_{Pl}, \quad (31)
 \end{aligned}$$

with $P(\beta)$ denoting the primordial power spectrum. Equation (31) only applies to flat and open universes, whereas for the closed universe, the eigenvalues of the Laplacian are discrete, so the integral is replaced with a sum over $K^{-1/2}\beta = 3, 4, 5 \dots$ ($K^{-1/2}\beta = 1, 2$ are pure gauge modes; Abbott & Schaefer 1986). The usual choice for the power spectrum is

$$P(\beta) \propto \frac{(\beta^2 - 4K)^2}{\beta(\beta^2 - K)}, \quad (32)$$

which has equal power in the curvature perturbation per logarithmic interval of k (Lyth & Stewart 1990; White & Bunn 1995). Note that in equation (31) one integrates over β instead of k (as in the flat case).

4. INTEGRAL SOLUTION

Having derived the Boltzmann equation for temperature and polarization in § 3.2, we proceed to derive the integral solution, which was the basis of the numerically efficient algorithm in flat space (Paper I). An alternative, more geometrical derivation of the integral solution is presented in the Appendix. In the flat case, the temperature and polarization multipoles can be written as a time integral of the product of a source term and a geometrical term, which is the solution of the sourceless Boltzmann equation. The geometrical term (given in terms of spherical Bessel functions in the flat case) becomes a function of two parameters in a nonflat universe, because of the additional scale in the

problem, the curvature of the universe. The source term can be expressed, as in the flat case, in terms of the photon, baryon, and metric perturbations. The main property of this solution remains unchanged: the source term is a slowly varying function of the wavenumber, while the geometrical term, which oscillates much more rapidly, does not depend on the specific cosmological model, except through its curvature.

To obtain the integral solution, it is useful to work in spherical coordinates. The unperturbed metric can be written as

$$ds^2 = a^2[-d\tau^2 + d\chi^2 + r^2(\chi)(d\theta^2 + \sin^2 \theta d\phi^2)], \quad (33)$$

where the coordinate χ is related to r by

$$r(\chi) \equiv \begin{cases} K^{-1/2} \sin K^{1/2}\chi, & K > 0, \\ \chi & K = 0, \\ (-K)^{-1/2} \sinh(-K)^{1/2}\chi, & K < 0. \end{cases} \quad (34)$$

In these coordinates the eigenfunctions of the Laplacian (eq. [2]) are given by

$$G_{\text{sph}}(\mathbf{x}) = \Phi_{\beta}^l(\chi) Y_{lm}(\mathbf{n}). \quad (35)$$

The radial functions $\Phi_{\beta}^l(\chi)$ are the so-called ultraspherical Bessel functions. From the expression for the Laplacian in spherical coordinates it follows that $\Phi_{\beta}^l(\chi)$ obey the following differential equation (Abbott & Schaefer 1986):

$$\frac{d^2 u_{\beta}^l}{d\chi^2} + \left[\frac{\beta^2 - l(l+1)}{r(\chi)^2} \right] u_{\beta}^l = 0, \quad (36)$$

where $u_{\beta}^l(\chi) = r(\chi) \Phi_{\beta}^l(\chi)$. In the flat case the solutions for $\Phi_{\beta}^l(\chi)$ reduce to the familiar spherical Bessel functions $j_l(k\chi)$. The derivative of an ultraspherical Bessel function can be written as (Abbott & Schaefer 1986)

$$\dot{\Phi}_{\beta}^l(\chi) = \frac{\beta}{2l+1} [l b_l \Phi_{\beta}^l(\chi) - (l+1) b_{l+1} \Phi_{\beta}^{l+1}(\chi)], \quad (37)$$

where the derivative is with respect to $\chi = \tau_0 - \tau$, so that $d\chi = -d\tau$. Comparing equations (30) and (37), we see that the ultraspherical Bessel functions and their derivatives are solutions of the Boltzmann hierarchy in the absence of scattering and gravity. One can thus make the following *Ansatz* to solve the Boltzmann hierarchy:

$$\begin{aligned}
 \Delta_{Tl}(\tau) &= \int_0^{\tau} d\tau' e^{-\kappa(\tau, \tau')} [\Phi_{\beta}^l(\tau - \tau') S_0(\tau') \\
 &\quad + \dot{\Phi}_{\beta}^l(\tau - \tau') S_1(\tau') + \ddot{\Phi}_{\beta}^l(\tau - \tau') S_2(\tau')]. \quad (38)
 \end{aligned}$$

Here, coefficients S_0 , S_1 , and S_2 were introduced because there are sources for $l = 0, 1, 2$ in equation (30). By simple substitution of equation (38) into equation (30), we obtain,

$$S_0 = \dot{\eta} + \dot{\kappa} \left(\Delta_{T0} + \frac{\Pi}{4b} \right), \quad S_1 = \dot{\kappa} \frac{v_b}{k}, \quad S_2 = \alpha + \frac{3\dot{\kappa}\Pi}{4k^2 b}. \quad (39)$$

The values of the ultraspherical Bessel functions and their derivatives for $\chi = 0$ are also needed in the calculation, $\Phi_{\beta}^l(0) = \delta_{l0}$, $\dot{\Phi}_{\beta}^l(0) = (k/3)\delta_{l1}$, and $\ddot{\Phi}_{\beta}^l(0) = 2/15(k^2 \bar{b} \delta_{l2}) - (k^2/3)\delta_{l0}$. These derivatives can be obtained from equation (37) using $\dot{\Phi}_{\beta}^l(0) = \delta_{l0}$.

Finally, integrating equation (38) by parts, one can eliminate the derivatives of ultraspherical Bessel functions, and

the solution can be written in the following form:

$$\Delta_{Tl} = \int_0^{\tau_0} d\tau \Phi_\beta^l(\tau_0 - \tau) S_T(\beta, \tau)$$

$$S_T(\beta, \tau) = g \left(\Delta_{T0} + 2\dot{\alpha} + \frac{\dot{v}_b}{k} + \frac{\Pi}{4\bar{b}} + \frac{3\ddot{\Pi}}{4k^2\bar{b}} \right) + e^{-\kappa(\dot{\eta} + \ddot{\alpha})} + \dot{g} \left(\frac{v_b}{k} + \alpha + \frac{3\dot{\Pi}}{4k^2\bar{b}} \right) + \frac{3\ddot{g}\Pi}{4k^2\bar{b}}, \quad (40)$$

where we have defined the visibility function $g = \kappa e^{-\kappa}$. Comparing this expression to the equivalent one for the flat universe (Paper I), one can see that the only difference in the present case is that Π is always divided by \bar{b} , which comes from the fact that $\Phi_\beta^2(0) = (2/15)k^2\bar{b}$, while $j_2(0) = (2/15)k^2$. Thus, to transform from the flat to the general solution, one should replace the Bessel functions with their nonflat generalization and introduce a factor of \bar{b} to account for the different normalization of these functions at the origin.

To solve the polarization hierarchy we use the recursion relation (Abbott & Schaefer 1986),

$$\sqrt{k^2 - K(l+1)^2} \Phi_\beta^{l+1}(\chi) = (2l+1) \cot_K(\chi) \Phi_\beta^l(\chi) - \sqrt{k^2 - Kl^2} \Phi_\beta^{l-1}(\chi), \quad (41)$$

where

$$\cot_K(\chi) \equiv \begin{cases} K^{1/2} \cot K^{1/2}\chi, & K > 0, \\ \chi^{-1}, & K = 0, \\ (-K)^{1/2} \coth(-K)^{1/2}\chi, & K < 0. \end{cases} \quad (42)$$

Using this and equation (37), one finds

$$\left(\frac{\Phi_\beta^l}{r^2} \right) = \frac{\beta}{2l+1} \left[(l-2)b_l \frac{\Phi_\beta^{l-1}}{r^2} - (l+3)b_{l+1} \frac{\Phi_\beta^{l+1}}{r^2} \right], \quad (43)$$

where the time derivative is taken on (Φ_β^l/r^2) . This means that Φ_β^l/r^2 solves the polarization free-streaming hierarchy equation (30) and is therefore the Green's function for polarization. The full solution is obtained by a substitution into equation (30):

$${}_2\Delta_{Pl} = - \int_0^{\tau_0} d\tau \frac{3g\Pi}{4} \frac{\Phi_\beta^l(\tau_0 - \tau)}{k^2 r^2 \bar{b}}. \quad (44)$$

An alternative derivation of this result and photon transport in general can be found in the Appendix.

Equations (40) and (44) are the main results of this section. The numerical implementation of these solutions lead to a significant reduction in computational time in the flat case. For this to be a successful strategy, we need to show that the ultraspherical Bessel functions can be computed efficiently. We turn to this subject next.

5. THE ULTRASPHERICAL BESSEL FUNCTIONS

The main difficulty in the numerical implementation of equations (40) and (44) is the calculation of the ultraspherical Bessel functions $\Phi_\beta^l(\chi)$. The method used in the flat case was to precompute and tabulate these functions for all the values of interest. This was feasible, because the functions only depend on the product $k\chi$. In the nonflat models, another scale is introduced in the problem, the curvature of the universe. The ultraspherical Bessel functions become

functions of both β and χ separately. Their tabulation is not feasible, because these functions are rapidly oscillating in both parameters, and an excessive amount of memory would be needed to store the functions sufficiently densely to assure accurate results. In this section we develop an efficient method for computing the functions rapidly and with the necessary accuracy for the purpose of CMB calculations.

The simplest approach for calculating the ultraspherical Bessel functions would be to use the recursion relation in equation (41). This method is usually recommended as the most efficient if only one particular value of $\Phi_\beta^l(\chi)$ is required (e.g., Press et al. 1992). Unfortunately, using this recursive method results in computational time that is significantly longer than the time needed to compute the source term, so that the total integration time becomes excessive. The main drawback of this method is that for every time step needed to compute the time integration in equation (40), all Φ_β^l are calculated up to the required l_{\max} . However, the smoothness of the C_l spectra allows us to calculate them sparsely and still obtain very accurate results. The structure of the integral solution in equation (40) does not couple different l modes, and one can use this property to reduce computational time significantly (Paper I). The second shortcoming of the recursive method is that one does not use the value of Φ_β^l at the previous time step, although, to guarantee accurate integration of equation (40) one needs to sample Φ_β^l sufficiently densely that differences between successive values are small. Both shortcomings suggest that one could efficiently compute the ultraspherical Bessel functions directly from the differential equation (36). Although this is not as efficient as the recursive method for any given time τ , it is much more efficient than the recursive method if one requires the values of the ultraspherical Bessel functions for a number of time steps between 0 and τ_0 . Moreover, one only needs to evaluate the functions at the needed values of l , which is typically every 50th value, if 1% accuracy is desired.

The structure of the ultraspherical Bessel functions is oscillatory and similar to the ordinary Bessel functions (Fig. 1). The differential equation (36) can be viewed as the Schrödinger equation for a particle with energy $E = \beta^2$ in a potential $V = l(l+1)/r(\chi)^2$. Thus, for χ such that $\beta r(\chi) > [l(l+1)]^{1/2}$, where the “energy” is greater than the “potential,” the solution is oscillatory. For $\beta r(\chi) < [l(l+1)]^{1/2}$, there is a growing and a decaying solution, $u_\beta^l \propto r^{l+1}$ and $u_\beta^l \propto r^{-l}$, respectively. The growing solution corresponds to $\Phi_\beta^l(\chi)$. In order to obtain an accurate numerical convergence, the integration needs to be started in the regime where $\Phi_\beta^l(\chi)$ is small, which in our case means beginning the integration close to $\beta r(\chi) \approx l$. The equation then needs to be evolved in the direction of increasing χ until recombination, where $\chi \sim \tau_0$. The integration of $\Phi_\beta^l(\chi)$ therefore proceeds in the opposite time direction from the evolution of Boltzmann, fluid, and Einstein equations (§ 2). If one were to start the integration at early times and evolve the Bessel functions to smaller radial distances χ (i.e., the present time), the integration would be numerically unstable, as the decaying $u_\beta^l \propto r^{-l}$ mode would increasingly contaminate the solution.

The starting value for the integration of equation (36) has to be chosen so that $\Phi_\beta^l(\chi)$ has some fixed small value, typically 10^{-6} . The function is changing rapidly for $\beta r(\chi) < [l(l+1)]^{1/2}$, so one cannot start just anywhere

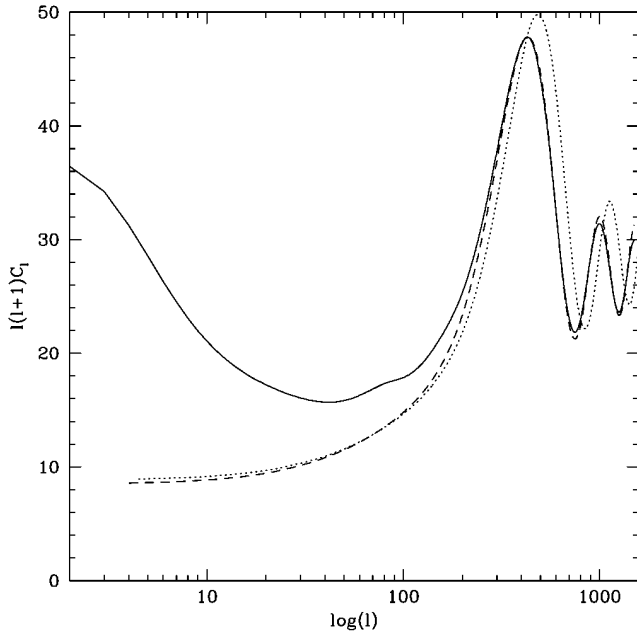


FIG. 1.—Comparison between ultraspherical Bessel function $\Phi_{\beta}^{100}(x)$ and spherical Bessel function $j_{100}(\beta \sin_K x)$ as a function of $\beta \sin_K x$. The two functions agree qualitatively, but $\Phi_{\beta}^{100}(x)$ oscillates much more rapidly and has a higher amplitude at first oscillation.

below this value, because one would soon be in the regime in which $\Phi_{\beta}^l(\chi)$ is excessively small and numerical round-off errors become intolerable. One could use equation (41) as a downward recursion for a given value of β where $\Phi_{\beta}^l(\chi)$ is of order 10^{-6} , but this leads to two difficulties. One is that, where $\Phi_{\beta}^l(\chi) = 10^{-6}$, the asymptotic expansion for $\Phi_{\beta}^l(\chi)$ is not necessarily valid, as χ might be too large, so starting values of χ based on the asymptotic expansion do not necessarily lead to the desired value of the ultraspherical Bessel function. More importantly, using the recursion relation only for one value of χ at each β still results in an excessive computational time. The solution is to precompute the starting values for integration on a grid of β and l and to interpolate between them for any given value. Because the ultraspherical Bessel functions are not oscillatory in this regime, accurate interpolation can be achieved with only a small number of precomputed values, typically 25 values of β for each l .

One can further reduce the computational time by using an asymptotic expansion for large radial distances χ , which is obtained by the WKB approximation applied to equation (36),

$$u_{\beta}^l \approx \frac{\sin [\Theta(\chi)]}{\beta[\beta^2 - l(l+1)/r(\chi)^2]^{1/4}}, \quad (45)$$

where

$$\Theta(\chi) \equiv \int^{\chi} d\chi \sqrt{\beta^2 - l(l+1)/r(\chi)^2} \approx \beta\chi + \epsilon. \quad (46)$$

Here ϵ is a constant phase that can be obtained analytically, but we choose it in such a way as to match the phase at the point where we switch from integrating equation (36) to the WKB approximation (eq. [45]). Sufficiently high accuracy is achieved by switching to the WKB approximation after 100 oscillations of u_{β}^l .

6. APPROXIMATIONS

In this section we compare the results of exact calculations with some of the approximations, both those already used in the literature and some based on the integral solution. The goal of this section is to estimate the accuracy of flat space approximations, which avoid the need for computing the ultraspherical Bessel functions and which were often used in the context of reconstruction of cosmological parameters from the CMB. To avoid dealing with the complicated structure of ultraspherical Bessel functions, one can compute the C_l spectrum for a flat model and then rescale it in l as a result of the change in the angular diameter distance to recombination and in the size of the acoustic horizon (e.g., Bond et al. 1994; Jungman et al. 1996; Hu & White 1996). The quantities determining the plasma sound horizon and its time evolution are $\Omega_b h^2$ and $\Omega_m h^2$, with Ω_b and Ω_m being the density of baryons and matter in units of critical density, respectively. If these two parameters are kept fixed, the only change in the spectra for small angular scales should arise from the change in the size of the acoustic horizon. On large angular scales, this approximation fails because of additional effects from the decay of the gravitational potential in the $\Omega_m \neq 1$ universe (integrated Sachs-Wolfe contribution), as well as curvature effects on the initial spectrum and on the radial eigenmodes. The simplest and most often used approximation is rescaling the spectrum by $\Omega_0^{-1/2}$ (e.g., Jungman et al. 1996) while keeping $\Omega_m h^2$ and $\Omega_b h^2$ fixed. The dependence of the acoustic horizon on Ω_0 is only poorly approximated by this scaling and leads to significant errors, as shown in Figure 2 for the case of $\Omega_0 = 0.2$. Clearly, this approximation is too inaccurate to be useful for numerical analysis.

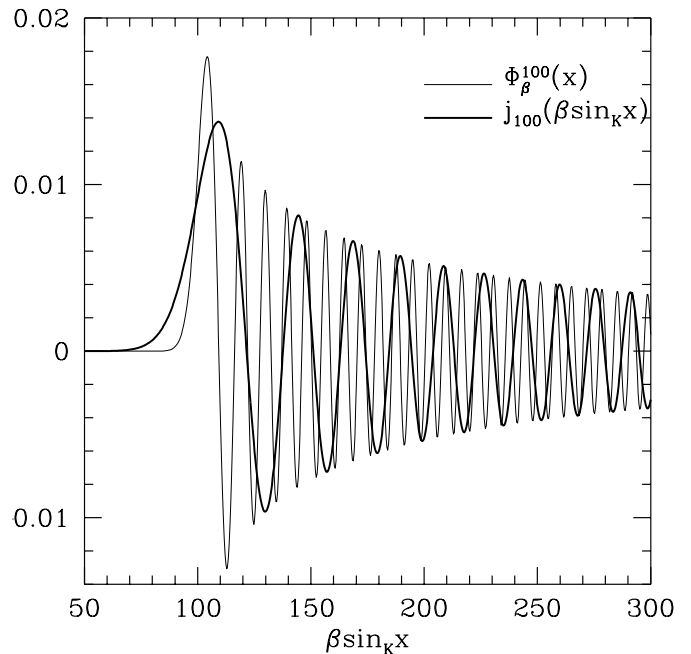


FIG. 2.—Comparison between the full calculation (solid line), $\Omega_0^{-1/2}$ rescaling of the flat spectrum (dotted line), and the angular diameter rescaling of the flat spectrum (dashed line) for the case with $\Omega_0 = 0.2$. The latter approximation fares significantly better than the first one on small scales, while on large scales, additional effects in open universes make the agreement poor for both approximations.

Significantly better is the approximation in which the angular diameter distance to the last scattering surface $r(\chi_r)$ is correctly calculated and then used to rescale the spectrum with (Hu & White 1996)

$$l = l^{\text{flat}} \frac{r(\chi_r)}{\chi_r}, \quad (47)$$

where χ_r is the radial distance to the recombination epoch. Recombination occurs roughly around $z \sim 1100$, but there is some uncertainty in its exact value, and it varies somewhat with Ω_b . The normalization of the spectrum is also a problem, since this scaling is only valid for sufficiently high values of l , making it impossible to use the lower multipoles for normalization. To avoid the two problems mentioned above, we performed the full open calculation and then shifted the flat spectra so that they agreed exactly at the first peak. This is therefore the most favorable case, and the above-mentioned difficulties will make the agreement worse. Figure 2 shows this approximation, together with the exact results. It obviously fails on large scales because of the effects mentioned above. While some of these effects can be modeled analytically, it is not obvious how one connects the small-scale and large-scale approximations. On small scales the agreement is significantly better, and the approximation deviates from the exact calculation by about 3%–4%. While this approximation fares significantly better than the other approximation above, it is still not sufficiently accurate for the forthcoming high-precision data.

We also tried a more sophisticated version of the above approximation that solves some of the problems. In this approximation one uses the integral solution and calculates the source term using equations presented in § 2, but the radial eigenfunctions are replaced with their flat-space approximations. This means replacing the ultraspherical Bessel functions in equation (40) by the spherical Bessel functions with the argument $kr(\chi)$, so that the appropriate angular diameter distance relation is used. The small-scale normalization and epoch of recombination are correctly calculated in this case, and the integrated Sachs-Wolfe term is included. If this were a good approximation, one could reduce the computational time by being able to tabulate the geometrical term as was done for the flat models (Paper I). While replacing the ultraspherical Bessel functions with the flat approximation gives qualitative agreement with the exact results, it *does not* converge to the exact solution in the limit of large l . This is shown in Figure 1, where the two are compared for $l = 100$. The approximation gives correct qualitative behavior and properly describes the position of the transition from $\Phi_\beta^l(\chi) \approx 0$ to the oscillatory regime, as well as the amplitude of oscillations. If the last scattering surface is thin, then in the time integration of equation (40) the spherical Bessel function does not change, and it can be taken out of the integral. Then, in equation (31) the square of the Bessel function is multiplied by the square of the source averaged over time; this product is integrated over the primordial spectrum. Because both the primordial spectrum and the source are slowly changing with k , this essentially amounts to an averaging of j_l^2 over its oscillation period. The result only depends on the amplitude and not on the oscillation frequency of the spherical Bessel function. This is the underlying reason why the approximation of rescaling the distance to the last scattering surface gives qualitative agreement in the final spectrum, and in particu-

lar, it correctly predicts the positions of the acoustic oscillation peaks.

However, as shown in Figure 1, the frequency of oscillation is different for the two functions, and this has important consequences when the finite width of the last scattering surface is taken into account. In this case one has to integrate the sources over the recombination epoch explicitly as in equation (40). The integrated Sachs-Wolfe term cannot be calculated correctly using this approximation, because the time dependence of the Bessel functions is important. This disagreement is most severe for the lower multipoles. The agreement for the part proportional to the visibility function is not good either, because $j_l[\beta \sinh(\chi)]$ oscillates faster in χ than Φ_β^l [the phase is proportional to $\beta \sinh(\chi)$, rather than to $\beta\chi$], so the damping is more severe than in its ultraspherical counterpart. The situation is even worse for the terms proportional to the first and second derivatives of the visibility function (eq. [40]). In the limit where the visibility function can be approximated by a δ -function, this is easy to understand. The derivatives of the visibility function act as derivatives of the δ -function, so these terms involve derivatives of the ultraspherical Bessel functions, which are not well approximated by the derivatives of $j_l(\beta \sinh \chi)$. This can be seen from the fact that the latter, although having the same amplitude as Φ_β^l , oscillate more rapidly. This problem could be solved by using equation (37) to express Φ_β^l in terms of the Φ_β^{l-1} and Φ_β^{l+1} , and approximating these by their flat counterparts. But the rest of the problems mentioned above will remain. This flat-space approximation is therefore not suitable for the integral approach, and its results are even worse than the simple rescaling of the spectrum with the angular diameter distance. To summarize the discussion, none of the flat-space approximations can match the exact results at better than 5% accuracy, which is not sufficient for the expected future observational precision.

7. IMPLEMENTATION

We are now in a position to present an efficient implementation of the method developed in the previous sections. Some of the technical issues of this implementation are identical to those in the flat case (Paper I) and will not be repeated here, but nonflat geometry also introduces some additional complications. The temperature spectra are calculated by integrating equation (40), while the source in this equation is obtained by integrating the equations presented in § 2. One of the advantages of calculating the C_l spectra this way is that the source in the integral only depends on the first few photon multipoles, so accurate results can be obtained by truncating the Boltzmann hierarchy at a very low value of l . As discussed in Paper I, this is only possible if one uses nonreflective boundary conditions to close the hierarchy in equation (30), so that the propagation of power from large scales to small scales is not reflected back onto the lowest moments of photon distribution. In the absence of scattering and integrated Sachs-Wolfe contribution, equation (30) becomes identical to equation (37); hence, one can use the recursion relation in equation (41) to relate Δ_{l+1} to Δ_l and thus to close the hierarchy. In reality, this relation is not exact, but since only the lowest moments need to be accurately calculated, one can use this closure scheme at some moment l_0 , which is sufficiently high so that any reflection of power from l_0 down to the lowest moments will be negligible. In practice, this is achieved to a high accuracy

for $l_0 = 7$, similar to the flat case. This therefore reduces the number of equations to be solved from a few thousand in the standard Boltzmann code to a few dozen in the integral approach, making the calculations significantly faster.

It was mentioned in the § 6 that the sources and the ultraspherical Bessel functions are calculated in the opposite directions of time, hence the integral in equation (40) cannot be computed at the same time as when the sources are computed. The radial eigenfunctions in equation (40) are calculated from equation (36) using a finite differencing scheme such as Runge-Kutta fourth-order integration, a procedure that automatically produces sufficient sampling points in time for an accurate integration. Because the sources do not depend on l , and, as discussed below, they need to be computed at far fewer points than the radial eigenfunctions, we compute them first at selected values of wavevector k by solving the system of equations presented in § 2. Their values are stored at selected time intervals. During the integration of equation (36), the sources are interpolated using cubic splines from their tabulated values, and equation (40) is solved simultaneously. To obtain an accurate interpolation of the sources, at most a few 100 values in time are needed, covering the time interval from recombination until today.

The main advantage of the integral method is in the sampling of the wavenumber k for the source term. The sources vary typically on a scale $k \sim 1/\tau_r$, where τ_r is the conformal time of recombination. The oscillations in Φ'_β are approximately 50 times faster, as they occur on a scale of the order of the inverse of the present conformal time τ_0 . We take advantage of this by calculating the sources at fewer values of k than that which is needed to sample properly the variations of the radial eigenfunctions and then interpolate them to obtain their values for the rest of the values of k . This reduces the number of k modes where the system of equations in § 2 is solved and is an important factor that enhances the performance of the method.

Because the C_l spectra are so smooth, they can be sampled in every 50th l , except for low values of l , for which denser sampling is needed. The rest of the C_l s are obtained by interpolation. This reduces the number of radial eigenfunctions that need to be computed, so that approximately 45 values of l are needed up to $l_{\max} = 1500$. They need to be sampled at least at a few points per oscillation, resulting in approximately 2000 points for the above l_{\max} . One therefore needs to solve 10^5 differential equations for the radial eigenmodes and only about 3000 differential equations for the source term. However, the differential equations for the sources are more complicated, so the actual computational time for the two terms is comparable. Typical CPU time for an open model with 1% accuracy up to $l_{\max} = 1500$ is about 60 s on an ALPHA-500 workstation, which is about 2 times slower than for a comparable model in a flat universe and orders of magnitude faster than any other method.

8. DISCUSSION

We derived the photon Boltzmann hierarchy for scalar temperature and polarization perturbations in a general

Robertson-Walker universe using a new expansion method in spin- s harmonics. Recently, a similar expansion has been presented by Hu & White (1997) and applied to scalar, vector, and tensor harmonics, but only in a flat universe. Combining these techniques will provide a complete treatment of cosmological perturbation theory in a perturbed Robertson-Walker universe and will be presented elsewhere (Hu et al. 1997). In this paper we concentrate on providing an efficient method for computing scalar CMB temperature and polarization anisotropies in a nonflat universe, generalizing the methods presented in Paper I. For this purpose we present an integral solution to the Boltzmann hierarchy equations. Temperature and polarization perturbations are written using Green's method as a time integral over the source term multiplied by a radial eigenfunction. The first term depends on the cosmological model, but not on the multipole moment, while the second depends only on the curvature of space and not on the rest of the cosmological parameters. This split clearly separates effects that depend on the source and those that depend on geometry, and it is more physically intuitive than the differential formulation. The numerical implementation of the integral method requires an efficient and accurate way of calculating the ultraspherical Bessel functions, because these cannot be stored in advance, as in the flat case. We achieve this by solving their differential equation. The implementation of the integral solution leads to a fast and accurate method for computing CMB anisotropy and polarization spectra with computational times of the same order as in the flat case. It should be noted that once the ultraspherical Bessel functions are calculated, computing vector and tensor spectra poses no further calculational difficulties.

The integral method presented in this paper can be used for studying theoretical predictions from various cosmological models with the purpose of comparing them to the real data. The implementation of the method is publicly available. The output of the calculation consists of both the temperature and polarization spectra, as well as the matter density power spectra, so one can use it to analyze both clustering and CMB data. In addition, an accurate small-scale normalization (σ_8) to the COBE data is provided by using the 4 yr analysis of the power spectrum (Bunn & White 1997). As such, it should replace various approximative methods used in the literature, if high precision is required. A new generation of experiments will be able to determine both the density power spectrum (e.g., Sloan Digital Sky Survey; 2dF survey) and the CMB spectrum (MAP; Planck) to an exquisite accuracy. The integral method presented here provides a tool for rapid and highly accurate analysis of theoretical models over a large range of parameter space. This should be useful in achieving a higher level of precision in the determination of the true cosmological model.

We acknowledge useful discussions with W. Hu, M. Mahachek, and M. White. We also want to thank the referee, Douglas Scott, for many useful comments. This work was partially supported by grant NASA NHG 5-2816.

APPENDIX A

In this Appendix we present an alternative and more intuitive derivation of the integral solution. We first present a solution of the photon free-streaming equation and then construct the general solution from it using Green's method. This method

clarifies the structure of the radial part of the integral solution and the connection between spatially varying perturbations and the resulting angular variation in the sky.

Polarization is described by $Q \pm iU$ that have spin $s = \pm 2$. The fields T , $Q \pm iU$ are functions of position in space specified in spherical coordinates by (χ, θ, ϕ) and direction in the sky. We take the observer to be located at the origin, in spherical coordinates at $\chi = 0$, so we are interested in T and $Q \pm iU$ as a function of the direction of observation \hat{n} at the origin today. As discussed in the main text, polarization is not only a function of \hat{n} , but also of the two directions perpendicular to \hat{n} , (\hat{e}_1, \hat{e}_2) , which are used to define the Stokes parameters. Thus,

$$T = T(\chi, \theta, \phi, \hat{n}, \tau), \quad Q \pm iU = (Q \pm iU)(\chi, \theta, \phi, \hat{n}, \hat{e}_1, \hat{e}_2, \tau). \quad (48)$$

We can make a single vector out of these quantities, $\mathcal{X} = (T, Q + iU, Q - iU)$.

We begin by considering the solution to the free-streaming equation,

$$\frac{d\mathcal{X}}{d\tau} = 0, \quad (49)$$

and then construct the complete solution from that. Notice that this is only true if the polarization vector does not rotate relative to $(\hat{e}_\theta, \hat{e}_\phi)$ during propagation, which can happen in some Bianchi models (Tolman & Matzner 1984). Given that the field $\mathcal{X}^*(\chi, \theta, \phi, \hat{n}, \hat{e}_1, \hat{e}_2, \tau^*) \equiv \mathcal{X}^*$ at some initial time τ^* , the free-streaming solution for the field at the origin today is simply

$$\mathcal{X}(0, \hat{n}, \hat{e}_\theta, \hat{e}_\phi, \tau_0) = \mathcal{X}^*(\chi^*, \theta, \phi, \hat{n}, \hat{e}_\theta, \hat{e}_\phi, \tau^*), \quad (50)$$

where (θ, ϕ) specify the direction of \hat{n} in spherical coordinates, and we use $(\hat{e}_\theta, \hat{e}_\phi) = (\hat{e}_1, \hat{e}_2)$. Because photon position and time are related via $\chi^* = \tau_0 - \tau^*$, we may drop the explicit dependence on τ^* in the following. When considering the perturbations produced by one single scalar mode, $G(x)$, the complete initial field $\mathcal{X}^* = (T^*, Q^* + iU^*, Q^* - iU^*)$ must be constructed from that scalar mode. The temperature is a spin-zero function of \hat{n} , so G and its radial derivatives can be used to construct the most general form of \mathcal{X}^* for this mode,

$$\Delta T^* = {}_0\epsilon_0 G + {}_0\epsilon_1 G_{|i} > \hat{n}^i + \dots, \quad (51)$$

where we introduced the coefficients ${}_0\epsilon_i$ to expand the temperature perturbation in terms of the mode functions and their derivatives. We concentrate on the first term, which corresponds to an initial distribution that is spatially varying as G and locally isotropic. It is through the free streaming of the photons that the spatial variations of the source create an angular-dependent distribution function, although it is isotropic initially. Taking G as the eigenfunction of the Laplacian in spherical coordinates, $G_{\text{sph}} = \Phi_\beta^l(\chi) Y_{lm}(\theta, \phi)$ (Abbott & Schaeffer 1986), we find, using equation (50),

$$\Delta T(0, \hat{n}, \tau_0) = {}_0\epsilon_0 \Phi_\beta^l(\tau_0 - \tau^*) Y_{lm}(\theta, \phi). \quad (52)$$

This means that $\Phi_\beta^l(\tau_0 - \tau^*)$ is a solution of the free-streaming equation, which we used in the main text to construct the full solution of the Boltzmann equation for temperature. The source terms for temperature consist not only of the isotropic term, but also of higher multipoles. Therefore, for the complete solution we have to include also the terms proportional to the derivatives of the ultraspherical Bessel functions, corresponding to higher order terms in the expansion of equation (51).

For polarization we need an initial field of spin 2, which is a function of \hat{n} and $(\hat{e}_\theta, \hat{e}_\phi)$. We can construct a function like this by contracting the derivatives of G with $\hat{m} = 2^{-1/2}(\hat{e}_\theta + i\hat{e}_\phi)$, $\hat{\bar{m}} = 2^{-1/2}(\hat{e}_\theta - i\hat{e}_\phi)$, and \hat{n} in the following way:

$$\begin{aligned} \Delta(Q + iU)^* &= {}_2\epsilon_0 G_{|ij} \hat{m}^i \hat{m}^j + {}_2\epsilon_1 G_{|ijk} \hat{m}^i \hat{m}^j \hat{n}^k + \dots, \\ \Delta(Q - iU)^* &= -{}_2\epsilon_0 G_{|ij} \hat{\bar{m}}^i \hat{\bar{m}}^j + -{}_2\epsilon_1 G_{|ijk} \hat{\bar{m}}^i \hat{\bar{m}}^j \hat{n}^k + \dots, \end{aligned} \quad (53)$$

where again we have introduced expansion coefficients ${}_2\epsilon_i$. For polarization we only need to consider the first term in each expansion, because this suffices for the angular structure of the source. The free-streaming solution is

$$\begin{aligned} \Delta(Q + iU)(0, \hat{n}, \hat{e}_\theta, \hat{e}_\phi) &= {}_2\epsilon_0 G_{|ij} \hat{m}^i \hat{m}^j, \\ \Delta(Q - iU)(0, \hat{n}, \hat{e}_\theta, \hat{e}_\phi) &= -{}_2\epsilon_0 G_{|ij} \hat{\bar{m}}^i \hat{\bar{m}}^j. \end{aligned} \quad (54)$$

By taking derivatives of $G_{\text{sph}}(x)$, we can show that

$$\begin{aligned} G_{\text{sph}|ij} \hat{m}^i \hat{m}^j &= \sqrt{(l+2)!/(l-2)!} \frac{\Phi_\beta^l(\chi)}{r(\chi)^2} {}_2Y_{lm}(\theta, \phi), \\ G_{\text{sph}|ij} \hat{\bar{m}}^i \hat{\bar{m}}^j &= \sqrt{(l+2)!/(l-2)!} \frac{\Phi_\beta^l(\chi)}{r(\chi)^2} -{}_2Y_{lm}(\theta, \phi), \end{aligned} \quad (55)$$

so that equation (54) becomes

$$\begin{aligned} \Delta(Q + iU)(0, \hat{n}, \hat{e}_\theta, \hat{e}_\phi) &= {}_2\epsilon_0 \sqrt{(l+2)!/(l-2)!} \frac{\Phi_\beta^l(\chi)}{r(\chi)^2} {}_2Y_{lm}(\theta, \phi), \\ \Delta(Q - iU)(0, \hat{n}, \hat{e}_\theta, \hat{e}_\phi) &= -{}_2\epsilon_0 \sqrt{(l+2)!/(l-2)!} \frac{\Phi_\beta^l(\chi)}{r(\chi)^2} -{}_2Y_{lm}(\theta, \phi), \end{aligned} \quad (56)$$

with $\chi = \tau_0 - \tau$. This shows that $\Phi_\beta^l/r(\chi)^2$ is the free-streaming solution for polarization, as was obtained using a different method in the main text.

The complete Boltzmann equation for polarization is of the form

$$\begin{aligned}\frac{d\Delta(Q + iU)}{d\tau} &= -\dot{\kappa} \Delta(Q + iU) - \frac{3\dot{\kappa}\Pi}{2k^2\bar{b}} G_{|ij} \hat{m}^i \hat{m}^j, \\ \frac{d\Delta(Q - iU)}{d\tau} &= -\dot{\kappa} \Delta(Q - iU) - \frac{3\dot{\kappa}\Pi}{2k^2\bar{b}} G_{|ij} \hat{m}^i \hat{m}^j.\end{aligned}\quad (57)$$

The $G_{|ij} \hat{m}^i \hat{m}^j$ leads to the usual $1 - \mu^2 \propto 1 - P_2(\mu)$ dependence of Thomson scattering. The angular dependence of the source is the simplest spin-two function that can be constructed from a scalar. One can interpret the above equation as stating that at each time τ^* , a contribution $d(\Delta Q + i\Delta U) \propto \dot{\kappa} \Pi G_{|ij} \hat{m}^i \hat{m}^j d\tau$ is generated, and then free streamed until today. If there is scattering along the way, only a fraction $\exp(-\kappa)$ of the photons reach the observer. Given the free-streaming solution (eq. [56]), the complete solution can be written as

$$\begin{aligned}\Delta(Q + iU)(0, \hat{n}, \hat{e}_\theta, \hat{e}_\phi, \tau_0) &= -\sqrt{\frac{(l+2)!}{(l-2)!}} \left[\int_0^{\tau_0} d\tau g(\tau) \frac{3\Pi\Phi_\beta^l(\tau_0 - \tau)}{4k^2\bar{b}r(\chi)^2} \right] {}_2Y_{lm}(\theta, \phi), \\ \Delta(Q - iU)(0, \hat{n}, \hat{e}_\theta, \hat{e}_\phi, \tau_0) &= -\sqrt{\frac{(l+2)!}{(l-2)!}} \left[\int_0^{\tau_0} g(\tau) \epsilon \frac{3\Pi\Phi_\beta^l(\tau_0 - \tau)}{4k^2\bar{b}r(\chi)^2} \right] {}_{-2}Y_{lm}(\theta, \phi),\end{aligned}\quad (58)$$

where $g(\tau)$ is the visibility function. When considering solutions of equation (30) corresponding to one mode that is the generalization of a single plane wave, a superposition of solutions (58) for all l with $m = 0$ must be used.

The above solutions for temperature and polarization help to illustrate the relation between the radial part of the mode function G and the free-streaming solution for \mathcal{X} as a function of angle in the sky. When we look in a given direction on the sky, we observe what was happening away from us at a distance $\chi = \tau_0 - \tau^*$. This couples the spatial variation of the mode functions with the angular variations of the observed distribution. The angular dependence of the sources, which is constrained by the spin nature of the variables, is also responsible for the specific form of the integral solution. The source for scalar polarization has to be constructed out of derivatives of the mode functions that change the radial dependence of the solution from Φ_β^l to Φ_β^l/r^2 .

These arguments can be extended to vector and tensor modes. The radial and angular dependence of the mode functions differs from the scalar case and can be found in Tomita (1982). In the case of temperature, the source is proportional to $h_{rr} = h_{ij} \hat{n}^i \hat{n}^j$, while for polarization, it is proportional to $h_{ij} \hat{m}^i \hat{m}^j$ and $h_{ij} \hat{m}^i \hat{n}^j$ for $Q + iU$ and $Q - iU$ for any type of perturbation. This, together with the explicit mode functions (Tomita 1982), can be used to verify the flat-space solution obtained previously (Zaldarriaga & Seljak 1997). Detailed analysis of vector and tensor nonflat Boltzmann equations will be presented elsewhere (Hu et al. 1997).

REFERENCES

- Abbott, L. F., & Schaefer, R. K. 1986, *ApJ*, 308, 546
 Bardeen, J. M. 1980, *Phys. Rev. D*, 22, 1882
 Bertschinger, E. 1996, in *Cosmology and Large Scale Structure*, ed. R. Schaefer et al. (Netherlands: Elsevier Science), 273
 Bond, J. R., et al. 1994, *Phys. Rev. Lett.*, 72, 13
 Bond, J. R., & Efstathiou, G. 1984, *ApJ*, 285, L45
 Bond, J. R., Efstathiou, G., & Tegmark, M. 1997 (astro-ph/9702100)
 Bucher, M., Goldhaber, A. S., & Turok, N. 1995, *Phys. Rev. D*, 52, 3314
 Bunn, E. F., & White, M. 1997, *ApJ*, 480, 6
 Chandrasekhar, S. 1960, *Radiative Transfer* (New York: Dover)
 Goldberg, J. N., et al. 1967, *J. Math. Phys.*, 8, 2155
 Gorski, K. M., et al. 1995, *ApJ*, 446, L67
 Gouda, N., & Sugiyama, N. 1992, *ApJ*, 395, L59
 Hu, W., Bunn, E., & Sugiyama, N. 1995, *ApJ*, 447, L59
 Hu, W., Seljak, U., White, M., & Zaldarriaga, M. 1997, *Phys. Rev. D*, in press
 Hu, W., & White, M. 1996, *ApJ*, 471, 30
 ———, 1997 (astro-ph 9702170)
 Jungman, G., Kamionkowski, M., Kosowsky, A., & Spergel, D. N. 1996, *Phys. Rev. D*, 54, 1332
 Kamionkowski, M., Kosowsky, A., & Stebbins, A. 1997, *Phys. Rev. D*, 55, 7368
 Kamionkowski, M., Spergel, D., & Sugiyama, N. 1994, *ApJ*, 426, L57
 Kochanek, C. S. 1996, *ApJ*, 473, 595
 Liddle, A. R., et al. 1995, *MNRAS*, 278, 644
 Lifshitz, E. M. 1946, *J. Phys. USSR*, 10, 16
 Lineweaver, C. H., Barbosa, D., Blanchard, A., & Bartlett, J. G. 1996 (astro-ph/9610133)
 Lyth, D. H., & Stewart, E. D. 1990, *Phys. Lett.*, B252, 336
 Ma, C.-P., & Bertschinger, E. 1995, *ApJ*, 455, 7
 Peebles, P. J. E. 1993, *Principles of Physical Cosmology*, (Princeton: Princeton Univ. Press)
 Peebles, P. J. E., & Yu, J. T. 1970, *ApJ*, 162, 815
 Perlmuter, S., et al. 1996, preprint (astro-ph/9608192)
 Press, W. H., Teukolsky, S. A., Vetterling, W. T., & Flannery, B. P. 1992, *Numerical Recipes in Fortran* (2d ed.; New York: Cambridge Univ. Press)
 Ratra, B., & Peebles, P. J. E. 1994, *ApJ*, 432, L5
 Rocha, G., & Hancock, S. 1996 (astro-ph/9611228)
 Seljak, U., & Zaldarriaga, M. 1996, *ApJ*, 469, 437 (Paper I)
 Smoot, G., et al. 1992, *ApJ*, 396, L18
 Tolman, B. W., & Matzner, R. A. 1984, *Proc. R. Soc. London A*, 392, 391
 Tomita, K. 1982, *Prog. Theor. Phys.*, 68, 310
 White, M., & Bunn, E. 1996, *ApJ*, 460, 1071
 White, M., & Scott, D. 1996, *ApJ*, 459, 415
 Wilson, M. L., & Silk, J. 1981, *ApJ*, 243, 14
 Zaldarriaga, M., & Seljak, U. 1997 *Phys. Rev. D*, 55, 1830
 Zaldarriaga, M., Spergel, D., & Seljak, U. 1996 (astro-ph/9702157)